R. ALROZI[1,2], N.A. ZUBIR[1,2,3*], N.F.A. BAKAR[4], J. MOTUZAS[5], N.H.H.A. BAKAR[6], D.K. WANG[7]

OXIDATIVE DEGRADATION KINETICS OF RECALCITRANT MACRO AND MICROPOLLUTANTS USING CaMFeO$_3$ (M = Cu, Mo, Co) PEROVSKITE CATALYST

Understanding the kinetics behavior of recalcitrant organic degradation in presence of catalyst is important in determining the reaction rates of catalysis. Therefore, this study investigates the kinetic behavior of oxidative degradation for different types of recalcitrant organic pollutants, namely as acid orange II (AOII) macropollutant and caffeine (CAF) micropollutant using B-site substituted CaMFeO$_3$ (M = Cu, Mo, Co) perovskite catalysts. The kinetic study was analyzed based on four kinetic models which are pseudo-zero-order, first-order, second-order and BMG. Interestingly, CaCuFeO$_3$ exhibited a unique kinetic behavior in which the reaction followed a different kinetic model: pseudo-second-order for AOII and pseudo-first-order for CAF. The reaction rate of CAF degradation in the presence of CaCuFeO$_3$ was increased by nine orders of magnitude (k = 1.8×10^{-3} min^{-1}) within 4 hr of reaction compared to pristine CaFeO$_3$ (k = 0.2×10^{-3} min^{-1}). On the contrary, CaFeO$_3$, CaMoFeO$_3$ and CaCoFeO$_3$ were fitted to BMG kinetic model for the CAF degradation. These results indicate that the partial substitution of B-site cation in the perovskite structure alters the catalytic reactivity of the resultant substituted perovskite catalysts and subsequently influences the overall kinetics behavior of the oxidative degradation in both recalcitrant macro and micropollutants.

Keyword: Kinetic; Perovskite Catalyst; B-site Cation; Macropollutant; Micropollutant

1. Introduction

Advanced oxidation processes (AOPs), such as Fenton reactions, photocatalytic oxidation, electrochemical oxidation reactions and ozone oxidation are being recognized as effective methods for wastewater treatment in degrading a wide range of recalcitrant organic pollutants [1,2]. Among all the available AOPs, Fenton oxidation is one of the most extensively utilized AOPs due to its rapid reaction rate and high oxidation capacity. The Fenton oxidation process involves a series of complex reactions with the main reaction of Fe^{2+} with H$_2$O$_2$, producing highly reactive hydroxyl radicals ($^{\bullet}$OH) (Eq. (1)). When the Fe^{3+} reacts with H$_2$O$_2$, it regenerates into Fe^{2+} and produces hydroperoxyl radicals ($^{\bullet}$OOH) (Eq. (2)) [3]. Most organic pollutants can be efficiently and non-selectively degraded by $^{\bullet}$OH radicals during catalysis due to its high redox potential (E^o = 2.80 V) [4].

$$Fe^{2+} + H_2O_2 \rightarrow Fe^{3+} + OH^- + HO^{\bullet} \qquad (1)$$

$$Fe^{3+} + H_2O_2 \rightarrow Fe^{2+} + H^+ + HO_2^{\bullet} \qquad (2)$$

Conventional Fenton oxidation is usually conducted under acidic conditions due to the tendency of Fe^{3+} to precipitate and lose its catalytic efficacy at high pH levels. However, maintaining the pH at acidity region could increase the expense of treatment and negatively impact soil and water quality [5,6]. Therefore, the heterogeneous Fenton/Fenton-like process has garnered significant interest due to its ability to overcome the limitations of the homogeneous Fenton process. In the heterogeneous Fenton/Fenton-like system, the catalytic reactions take place within the vicinity of active sites on the surface of the solid catalyst, avoiding the leaching of iron ions, extending the operating pH range (including natural pH value of water), minimizing the generation of iron sludge and facilitating facile catalyst's recovery [7-9].

[1] CHEMICAL ENGINEERING STUDIES, COLLEGE OF ENGINEERING, UNIVERSITI TEKNOLOGI MARA, CAWANGAN PULAU PINANG, 13500, PERMATANG PAUH, PULAU PINANG, MALAYSIA
[2] HYBRID NANOMATERIALS, INTERFACES & SIMULATION (HYMFAST), CHEMICAL ENGINEERING STUDIES, COLLEGE OF ENGINEERING, UNIVERSITI TEKNOLOGI MARA, CAWANGAN PULAU PINANG, 13500, PERMATANG PAUH, PULAU PINANG, MALAYSIA
[3] WATER RESEARCH AND ENVIRONMENTAL SUSTAINABILITY GROWTH (WAREG), UNIVERSITI MALAYSIA PERLIS (UNIMAP), 02600 ARAU, PERLIS, MALAYSIA
[4] SCHOOL OF CHEMICAL ENGINEERING, COLLEGE OF ENGINEERING, UNIVERSITI TEKNOLOGI MARA SHAH ALAM, 40450 SHAH ALAM, SELANGOR, MALAYSIA
[5] THE UNIVERSITY OF QUEENSLAND, FIM2LAB-FUNCTIONAL INTERFACIAL MATERIALS AND MEMBRANES LABORATORY, SCHOOL OF CHEMICAL ENGINEERING, BRISBANE, QLD 4072, AUSTRALIA
[6] NANOSCEINCE RESEARCH LABORATORY, SCHOOL OF CHEMICAL SCIENCES, UNIVERSITI SAINS MALAYSIA, 11800 PENANG, MALAYSIA
[7] SCHOOL OF CHEMICAL AND BIOMOLECULAR ENGINEERING, THE UNIVERSITY OF SYDNEY, NEW SOUTH WALES, 2006, AUSTRALIA

* Corresponding author: noraida709@uitm.edu.my

As a result, many heterogeneous Fenton/Fenton-like catalysts have been developed, including metal-organic frameworks [10,11], graphene oxide [12,13] and mixed oxides such as perovskites [14-17], while the latter is typically preferable for environmental heterogeneous catalysis application.

Perovskite (ABO_3) is a type of crystalline ceramic that is classified in a group of mixed oxides. A-site represents an alkaline-earth metals or rare-earth metals, while B-site represents a transition metal. The physiochemical properties of the perovskite can be deliberately tailored by substituting different elements at the A and/or B sites, which are able to modulate the overall catalytic performances for the degradation of organic pollutants. Recent studies have shown that an improvement in catalytic performance as well as degradation kinetics rate was observed when different types of cations in the B-site either partially or fully substituted in the perovskite structure. For instance, Rao et. al. [18] introduced Cu-substituted $LaFeO_3$ ($LaFe_{0.925}Cu_{0.075}O_{3-\delta}$) for sulfadiazine degradation, which showed that substitution of foreign cation into the B-site significantly increased the reaction kinetic constant from 0.0759 min^{-1} for $LaFeO_3$ to 0.3829 min^{-1} for $LaFe_{0.925}Cu_{0.075}O_{3-\delta}$. Meanwhile, Xie et. al. [19] reported that the enhancement of redox activity between Co and Cu in $LaCo_{0.4}Cu_{0.6}O_{3-\delta}$ facilitated the activation of H_2O_2 to $HO^\bullet$ radicals, which led to a complete degradation of ciprofloxacin (CIP) within 2 hr of reaction time. The reaction kinetic constant value of CIP degradation by $LaCo_{0.4}Cu_{0.6}O_{3-\delta}$ ($k = 0.03945$ min^{-1}) was 2.5 times higher than that of $LaCoO_3$. Gao et. al. [20] also achieved a complete degradation of sulfamethoxazole over Cu substituted in $LaMnO_3$ and the reaction kinetic constant ($k = 0.2001$ min^{-1}) enhanced by 8.3 times as compared to $LaMnO_3$. Based on the above discussions, the degradation of recalcitrant emerging micropollutants by B-site substituted perovskite structure mainly followed the first order reaction kinetic model. Similar behaviors of first order kinetic model by other B-site substituted perovskite catalysts for oxidative degradation of recalcitrant micropollutants were also observed elsewhere [21-23]. Nevertheless, it is necessary to evaluate the impact of partial substitution of B-site cation on the degradation reaction rate constants of organic pollutants using different kinetic models. In-depth understanding of laboratory-scale kinetic models is crucial to gaining detailed insights into chemical reactions, optimizing reaction conditions, and ensuring the safety that warrants efficient and sustainable industrial practice.

Hence, the present work aims to evaluate the oxidative degradation kinetics of recalcitrant macro and micropollutants using $CaMFeO_3$ (M = Cu, Mo, Co) perovskite catalysts using different types of kinetic models (pseudo-zero-order, first-order, second-order and BMG-Behnajady, Modirshahla, and Ghanbary). The kinetic study of the macropollutant (acid orange II (AOII)) was performed using data from previous work [15], while caffeine (CAF) was chosen as the model micropollutant because it is considered as the most widely consumed psychoactive drugs globally, with an estimated consumption of about 120,000 tonnes annually [24,25]. CAF is also known as the most frequently detected pharmaceutically active compounds in the aquatic environment [26], and conventional waste water treatment plants are not able to effectively degrade CAF, which can give adverse effect to human and aquatic life after long-term exposure. The reactivity of $CaMFeO_3$ (M = Cu, Mo, Co) perovskite catalysts on CAF degradation and the reaction kinetic models for both AOII macropollutant and CAF micropollutant were discussed in this study.

2. Material and experimental procedure

2.1. Materials

Calcium nitrate tetrahydrate ($Ca(NO_3)_2.4H_2O$; ≥99%), iron(III) nitrate nonahydrate ($Fe(NO_3)_3.9H_2O$; 99%), ammonium molybdate (($NH_4)_2MoO_4$; 99%), cobalt(II) chloride hexahydrate ($CoCl_2.6H_2O$; 98%), copper(II) nitrate trihydrate ($Cu(NO_3)_2.2.5H_2O$; ≥99%), ethylenediaminetetraacetic acid (EDTA), ammonium hydroxide (NH_4OH) solution, hydrogen peroxide (H_2O_2; 30% (w/w)), acid orange II (AOII), caffeine (CAF) (99%) and methanol for liquid chromatography (LiChrosolv® Reag. Ph Eur; 99%) were supplied by Sigma Aldrich. Citric acid monohydrate ($C_6H_8O_7.H_2O$; ≥99%) was purchased from QReC (Asia). All chemicals were of analytical grade and used as received without further purification.

2.2. Synthesis of B-site substituted $CaMFeO_3$ (M = Mo, Co, Cu) perovskite catalysts

The series of B-site substituted $CaMFeO_3$ (M = Mo, Co, Cu) perovskites was synthesized via EDTA-citric acid complexation method. Each A-site and B-site cation molar concentration was fixed at 0.05 M. A set of molar ratios of A-site precursor: B'-site precursor: B-site precursor: ethylenediamine tetra-acetic acid (EDTA): citric acid: ammonium hydroxide was kept constant at 1:1:1:1.1:2:10. For instance, in the synthesis of $CaMoFeO_3$ catalyst, 0.05 M $Ca(NO_3)_2.4H_2O$, 0.05 M $FeCl_3.6H_2O$, 0.05 M ($NH_4)_2MoO_4$ and 0.1 M $C_6H_8O_7.H_2O$ solutions were mixed and stirred for 15 min at the beginning. Then, a solution mixture containing 0.05 M NH_4OH and 0.055 M EDTA was added to the former mixture and stirred for 15 min at room temperature until well mixed.

Subsequently, the resultant homogeneous mixture was heated at 100°C under stirring to evaporate water to form a viscous solution. Further gelation of the viscous solution was carried out in the oven at 90°C for 24 hr. The dried gel samples then underwent a two-stage calcination process in a muffle furnace: first stage at 450°C for 8 h and second stage at 800°C for 4 h at a ramping rate of 5°C min^{-1} in air. The resultant $CaMoFeO_3$ perovskite was ground and stored prior to further use. Similar procedures were repeated for other B-site substituted perovskite catalysts using copper and cobalt precursors to synthesize $CaCuFeO_3$ and $CaCoFeO_3$, respectively. In addition, $CaFeO_3$ was also synthesized as a pristine unsubstituted B-site catalyst for comparison purposes.

2.3. Catalytic performances and kinetic analysis

The catalytic activities of the B-site substituted CaMFeO$_3$ perovskite catalysts were evaluated in oxidative degradation of AOII [15] and CAF. In the experiments on the oxidative degradation of CAF, 0.02 g of catalyst was dispersed in 100 mL of CAF solution in the presence of 22 mM H$_2$O$_2$ and stirred at 200 rpm for 4 hr at room temperature. At regular intervals, 5 mL of reaction suspension was withdrawn and filtered through a 0.2 μm filter syringe. The concentration of CAF supernatant solution was determined by high-performance liquid chromatography (HPLC) (Waters 2707 Autosampler) equipped with a XTERRA® RP18 column (4.6 mm × 250 mm, 5 μm). The wavelength of photodiode array detector (PDA) was 275 nm for caffeine. The mobile phase was selected as methanol and ultrapure water (40/60; v/v) and the injection volume was 10 μL. The reaction was quenched by the addition of 50μL of 1.0 M sodium thiosulfate (Na$_2$S$_2$O$_3$) into the CAF supernatant solution, prior to HPLC analysis.

The kinetic evaluation of oxidative degradation for both recalcitrant organics pollutants were investigated using pseudo-zero-order, first-order, second-order and BMG-Behnajady, Modirshahla, and Ghanbary [27] kinetic models. Pseudo-zero-order, first-order and second-order kinetic models are defined according to Eqs. (3)-(5), respectively:

$$C_t = C_o - k_o t \tag{3}$$

$$\ln C_t = \ln C_o - k_1 t \tag{4}$$

$$\frac{1}{C_t} = \frac{1}{C_o} + k_2 t \tag{5}$$

The k_o (mg L^{-1} min^{-1}), k_1 (min^{-1}), and k_2 (L mg^{-1} min^{-1}) are apparent kinetic rate constants of pseudo-zero-order, first-order, and second-order models, respectively, t is reaction time, and C_t is the pollutant concentration at a given time t.

The BMG model is written as in Eq. (6):

$$\frac{t}{\left[1 - \left(\dfrac{C_t}{C_o}\right)\right]} = m + bt \tag{6}$$

Where m and b are two constants respecting to initial oxidation capacities and reaction kinetics, respectively [27].

3. Results and discussion

3.1. Catalytic performances and kinetic analysis

Reactivity of CaMFeO$_3$ (M = Cu, Mo, Co) perovskite catalysts in the oxidation of acid orange II (AOII) macropollutant has been investigated in our previous works [15]. The AOII degradation data is summarized in TABLE 1. From TABLE 1, it was found that CaCuFeO$_3$ exhibited the most effective AOII degradation, with a rate of 97%, followed by CaMoFeO$_3$ at

90%, CaFeO$_3$ at 64%, and CaCoFeO$_3$ at 40%, within 60 min reaction time in the presence of H$_2$O$_2$. Such finding reveals that the enhanced AOII degradation in the presence of CaCuFeO$_3$ perovskite catalyst during catalysis was attributed to the facile generation of •OH radicals due to fast redox cycling of active sites (≡Cu$^+$/≡Cu^{2+} and ≡Fe^{2+}/≡Fe^{3+}). The fast redox cycling of the active sites can be well correlated with the magnitude resistance of the electron transfer mobility during catalysis. Interestingly, the magnitude of the resistance for CaCuFeO$_3$ was the lowest (~404 Ω) compared to others substituted perovskite catalysts as reported elsewhere [15].

TABLE 1

Data of AOII degradation in presence of CaFeO$_3$, CaCuFeO$_3$, CaMoFeO$_3$ and CaCoFeO$_3$ perovskite catalysts

Catalyst	Degraded AOII at 60 min		
	Absorbance	$C_{AOII,t}$ (mg/L)	AOII degradation (%)
CaFeO$_3$	0.5566	12.18	64%
CaCoFeO$_3$	0.9427	20.63	40%
CaMoFeO$_3$	0.1534	3.36	90%
CaCuFeO$_3$	0.0457	1.00	97%

Note: Experimental conditions: $C_{AOII,o}$ = 35 mg L^{-1}; H$_2$O$_2$ = 22 mM; Catalyst = 1.0 g L^{-1}; and unadjusted pH solution.
Calibration curve: Abs = 0.0457C_{AOII}, R^2 = 0.9998

In this study, the catalytic performances of CaMFeO$_3$ (M = Cu, Mo, Co) perovskite catalysts were tested for CAF micropollutant and the degradation profiles are shown in Fig. 1. Similar catalyst's reactivity trend was also observed for CAF degradation in the presence of H$_2$O$_2$. The catalyst's reactivity are as follows: CaCuFeO$_3$ (36%) > CaCoFeO$_3$ (24%) > CaMoFeO$_3$ (15%) > CaFeO$_3$ (10%). It was found that, after 60 min of reaction, CaFeO$_3$ perovskite catalyst was found to be completely deactivated, while the catalytic activity of both CaMoFeO$_3$ and
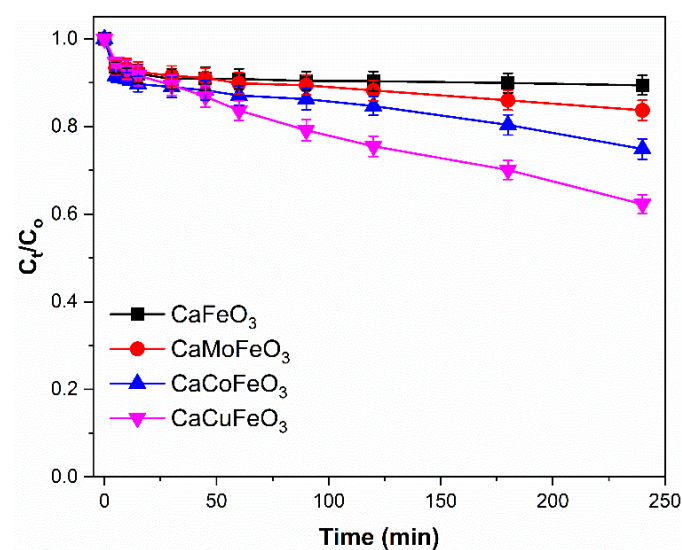
Fig. 1. Degradation profile of CAF in presence of CaFeO$_3$, CaCuFeO$_3$, CaMoFeO$_3$ and CaCoFeO$_3$ perovskite catalyst. Experimental conditions: CAF = 10 mg L^{-1}; H$_2$O$_2$ = 22 mM; Catalyst = 0.2 g L^{-1}; unadjusted pH and T = 27°C

CaCoFeO$_3$ were started to slowly deactivate until 4hr of catalysis. In contrast, CaCuFeO$_3$ was able to sustain its reactivity throughout the 4 hr of catalysis until it reached 36% degradation. Such findings suggest the efficient generation of $^{\bullet}$OH radicals facilitated by the regeneration of active site ($\equiv$Cu$^+$ and $\equiv$Fe$^{2+)}$) during catalysis. The effective redox cycles between $\equiv$Fe^{2+}/$\equiv$Cu$^+$ and $\equiv$Fe^{3+}/$\equiv$Cu^{2+} promote the efficient generation of $^{\bullet}$OH radicals, resulting in a much higher rate of CAF removal. It is interesting to note that the catalytic performance of CaCuFeO$_3$ in this work surpassed the CAF degradation reported by Simsek et. al [28] using LaFeO$_3$ perovskite catalyst and H$_2$O$_2$ as oxidant during dark catalysis.

Fig. 2 shows the chromatogram of CAF degradation in the presence of CaMFeO$_3$ (M = Cu, Mo, Co) perovskite catalysts at different reaction time. The chromatogram peak area appeared at retention time (RT) of 4.17 min represents the quantity or the concentration of CAF in the solution. The CAF chromatogram peak area decreased in the sequence of CaFeO$_3$ > CaMoFeO$_3$ > CaCoFeO$_3$ > CaCuFeO$_3$ at 4hr of reaction, which proved the CAF degradation profile as displayed in Fig. 1. The chromato-
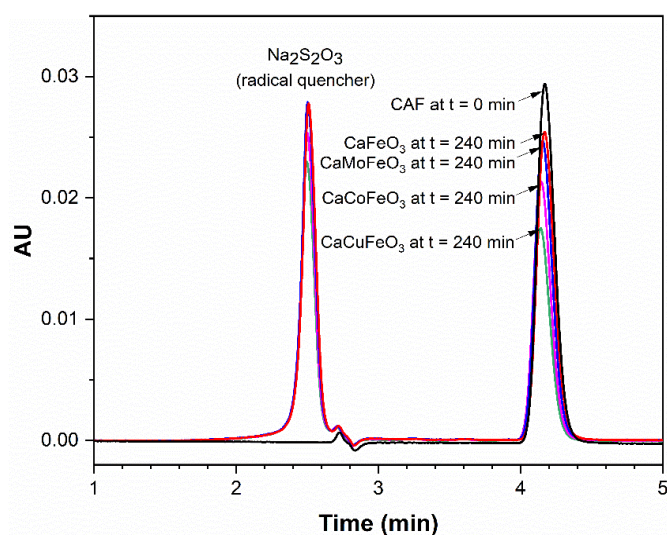
Fig. 2. Chromatogram of CAF during oxidative degradation using CaFeO$_3$, CaCuFeO$_3$, CaMoFeO$_3$ and CaCoFeO$_3$ at 4 hr of reaction time. Experimental conditions: CAF = 10 mg L^{-1}; H$_2$O$_2$ = 22 mM; Catalyst = 0.2 g L^{-1}; unadjusted pH and T = 27°C

gram peak at RT of 2.503 min indicates the presence of Na$_2$S$_2$O$_3$ as radical quencher to stop the reaction prior to HPLC analysis.

The kinetics behaviors of both AOII (Fig. 3) and CAF oxidation (Fig. 4) by CaMFeO$_3$ (M = Cu, Mo, Co) perovskite catalysts at unadjusted pH were further analyzed using four kinetic models (pseudo-zero-order, first-order, second-order and BMG). The results of correlation coefficients (R^2), apparent kinetic constants of the pseudo-zero-order, first-order, second-order (k_o, k_1 and k_2) and kinetics' parameters obtained on the BMG model ($1/m$ and $1/b$) for both AOII and CAF oxidation are shown in TABLE 2. As illustrated in TABLE 2, the pseudo-second order kinetic model fitted well to the AOII oxidation by all CaMFeO$_3$ (M = Cu, Mo, Co) perovskite catalysts, as it obtained higher R^2 values than the zero-order, first-order and BMG kinetic models. On the contrary, distinctive kinetic behavior was observed in the oxidative degradation of CAF. Only CaCuFeO$_3$ followed the pseudo-first order kinetic model, whereas CaFeO$_3$, CaMoFeO$_3$ and CaCoFeO$_3$ conformed to the BMG kinetic model. This result indicates that the degradation kinetics of heterogeneous catalysis was mainly influenced by the nature of recalcitrant organic pollutant in presence of perovskite catalyst.

For instance, the kinetic behavior profile of the CaCuFeO$_3$ perovskite catalyst showed a dependence on the molecular size and the dissociation constant (pK_a) of the recalcitrant organic pollutant. The oxidative degradation of the macropollutant (AOII dye) can be well described by the pseudo-second-order kinetic model, while the pseudo-first-order kinetic model applies to the micropollutant (CAF) (Fig. 5). The pK_a value of AOII and CAF is 11.4 [29] and 10.4 [30], respectively. These molecules are present in neutral or protonated form when pH of the solution is lower than the pK_a [31]. At the unadjusted pH of reaction mixture (pH 6.4), AOII molecules (1.25-1.27 nm [32]) tend to dissociate by deprotonation of the -NH-N= groups due to weak acidic strength [29], which subsequently leads to electrostatic repulsion between AOII and the negative-charge of CaCuFeO$_3$ perovskite catalyst [15]. Therefore, the oxidative degradation of AOII is likely associated with a possible combination of interactions [29] between the concentration of oxidant (H$_2$O$_2$) to be activated into $^{\bullet}$OH radicals and the concentration of AOII during heterogeneous catalysis. This interaction is

TABLE 2

Apparent kinetic rate constants of the zero-order (k_0), first-order (k_1), and second-order (k_2), kinetics' parameters obtained on the BMG model ($1/m$ and $1/b$) and correlation coefficients (R^2) obtained after data fits for AOII (60 min) and CAF (4 hr) oxidation

Pollutant	Catalyst	Zero Order		First Order		Second Order		BMG				
		k_o (mg L^{-1} min^{-1})	R^2	k_1 (min^{-1})	R^2	k_2 (L mg^{-1} min^{-1})	R^2	m	$1/m$ (min^{-1})	b	$1/b$	R^2
AOII	CaFeO$_3$	0.3238	0.8766	0.0161	0.9629	0.0009	0.9920	17.6056	0.0568	1.3770	0.7262	0.9181
	CaMoFeO$_3$	0.3957	0.6083	0.0359	0.8690	0.0045	0.9937	4.5475	0.2199	1.0472	0.9549	0.9908
	CaCoCoO$_3$	0.2031	0.8580	0.0077	0.9109	0.0003	0.9221	27.6243	0.0362	2.2272	0.4490	0.9205
	CaCuFeO$_3$	0.4942	0.6755	0.0613	0.9012	0.0192	0.9254	2.0404	0.4901	0.9996	1.0004	0.9236
CAF	CaFeO$_3$	0.0022	0.6596	0.0002	0.7723	0.00003	0.7852	238.0952	0.0042	9.6805	0.1033	0.9944
	CaMoFeO$_3$	0.0045	0.7304	0.0005	0.7863	0.00005	0.8211	153.8462	0.0065	6.3412	0.1577	0.9450
	CaCoCoO$_3$	0.0073	0.8314	0.0008	0.8624	0.00010	0.8880	128.2051	0.0078	4.1929	0.2385	0.9167
	CaCuFeO$_3$	0.0141	0.9565	0.0018	0.9930	0.00020	0.9910	59.88024	0.0167	2.4160	0.4139	0.8398
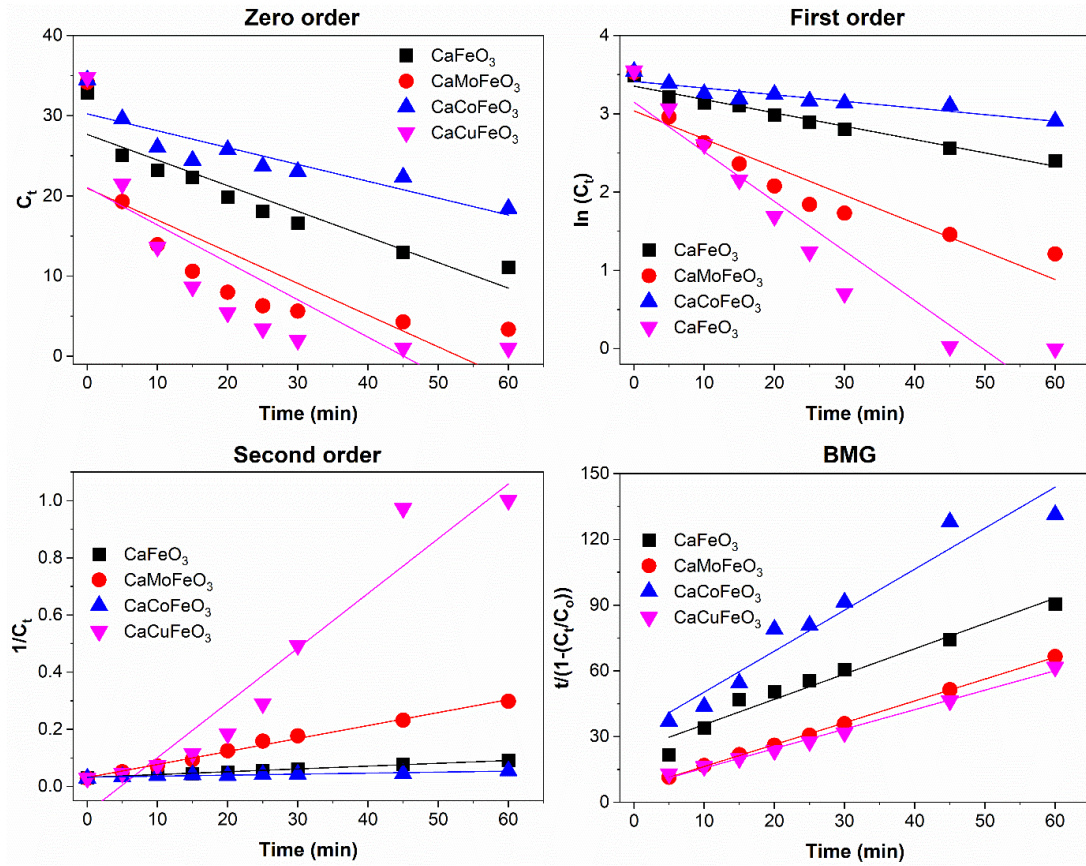
Fig. 3. AOII oxidative degradation in presence of B-site substituted CaMFeO$_3$ (M = Mo, Co, Cu) perovskite catalysts using different kinetic models. Experimental conditions: AOII = 35 mg L^{-1}; H$_2$O$_2$ = 22 mM; Catalyst = 1.0 g L^{-1}; unadjusted pH and T = 27°C

Fig. 4. CAF oxidative degradation in presence of B-site substituted CaMFeO$_3$ (M = Mo, Co, Cu) perovskite catalysts using different kinetic models. Experimental conditions: CAF = 10 mg L^{-1}; H$_2$O$_2$ = 22 mM; Catalyst = 0.2 g L^{-1}; unadjusted pH and T = 27°C

Fig. 5. Proposed profile of kinetics behavior for oxidative degradation of (a) AOII and (b) CAF in presence of $CaCuFeO_3$ perovskite catalysts

consistent with the observed principles of the pseudo-second-order kinetic model.

On the other hand, although the dissociations of CAF molecules (0.36 nm [33]) can occur in protonated form, the CAF molecules prone to predominate in neutral form [34] at an unadjusted pH of the reaction mixture (pH 6.9). Therefore, CAF molecules tend to be slightly pre-adsorbed within the vicinity of catalyst via the dipole-dipole interaction [35]. These interactions indicate that the oxidative degradation of CAF mainly depends on the activation of H_2O_2 into $^•OH$ radicals since the reaction occurs at the solid-liquid interfaces of $CaCuFeO_3$ perovskite catalysts. The reaction rate of CAF oxidation in the presence of $CaCuFeO_3$ catalyst was increased by ninefold ($k = 1.8 \times 10^{-3}$ min^{-1}) compared to pristine $CaFeO_3$ (k = 0.2×10^{-3} min^{-1}) within 4 hr of reaction, which can be attributed to fast redox cycling of the active sites ($\equiv Cu^+/\equiv Cu^{2+}$ and $\equiv Fe^{2+}/\equiv Fe^{3+}$) to generate $^•OH$ radicals during heterogeneous catalysis.

The reactions of $CaFeO_3$, $CaMoFeO_3$ and $CaCoFeO_3$ on CAF degradation that followed BMG kinetic model may exhibit the characteristics of Fe^{2+}/H_2O_2 system through Fenton process. According to Santana et. al [36], the BMG model can be represented by Fe^{2+}/H_2O_2 system kinetics that involve a two-stage pattern, consisting of an initial rapid stage followed by a subsequent slower stage. The rapid stage is ascribed to the interaction between Fe^{2+} and H_2O_2 that can be represented by the reciprocal of m ($1/m$). Interestingly, the highest initial degradation rate ($1/m = 0.0167$) was demonstrated by $CaCuFeO_3$, compared to $CaCoFeO_3$ ($1/m = 0.0078$), $CaMoFeO_3$ ($1/m = 0.0065$) and $CaFeO_3$ ($1/m = 0.0042$).

Meanwhile, the slower stage is caused by the accumulation of Fe^{3+} and a limited regeneration of Fe^{2+} by H_2O_2 that can be correlated with the reaction kinetics (b). The reciprocal of b ($1/b$) is also known as the maximum oxidation capacity which indi-

cates the highest possible degradation of organic pollutant that can be attained at infinite reaction time [27,30,35]. It is noteworthy that $CaCuFeO_3$ showed the highest value ($1/b = 0.4139$), followed by $CaCoFeO_3$ ($1/b = 0.2385$), $CaMoFeO_3$ ($1/b = 0.1577$) and $CaFeO_3$ ($1/b = 0.1033$). Similar behavior was also being observed in previous studies with different types of dye macropollutants [27,29,31,32] as well as 2,4-dichlorophenoxyacetic acid [41] and tetracycline micropollutants [42].

4. Conclusions

In summary, the B-site substituted $CaCuFeO_3$ perovskite catalyst exhibits a distinctive kinetic behavior in which the degradation followed a different kinetic model: pseudo-second-order for AOII and pseudo-first-order for CAF. Interestingly, the reaction rate of CAF degradation was increased by the nineth order of magnitude in the presence of $CaCuFeO_3$ ($k = 1.8 \times 10^{-3}$ min^{-1}) compared to pristine unsubstituted $CaFeO_3$ ($k = 0.2 \times 10^{-3}$ min^{-1}) perovskite catalyst. In contrast, CAF degradation by $CaFeO_3$, $CaMoFeO_3$ and $CaCoFeO_3$ were fitted to the BMG kinetic model that imparts different characteristics of catalytic behavior. These findings provide interesting insights into the reaction kinetics model and reactivity associated with various B-site cation substitutions within the structure of perovskite for recalcitrant macro and micropollutants.

REFERENCES

[1] D. Ma, H. Yi, C. Lai, X. Liu, X. Huo, Z. An, Critical review of advanced oxidation processes in organic wastewater treatment. Chemosphere **275**, 130104 (2021).
DOI: https://doi.org/10.1016/j.chemosphere.2021.130104

[2] Z.U.H. Khan et al., Removal of organic pollutants through hydroxyl radical-based advanced oxidation processes. Ecotoxicol. Environ. Saf. **267**, 115564 (2023).
DOI: https://doi.org/10.1016/j.ecoenv.2023.115564

[3] Y. Zhu et al., The differences in heterogeneous Fenton catalytic performance and mechanism of various iron minerals and their influencing factors: A review. Sep. Purif. Technol. **325**, 124702 (2023). DOI: https://doi.org/10.1016/j.seppur.2023.124702

[4] O. Legrini, E. Oliveros, A.M. Braun, Photochemical Processes for Water Treatment. Chem. Rev. **93,** 2, 671-698 (1993).
DOI: https://doi.org/10.1021/cr00018a003

[5] M. Usman, S. Jellali, I. Anastopoulos, Y. Charabi, B.H. Hameed, K. Hanna, Fenton oxidation for soil remediation: A critical review of observations in historically contaminated soils. J. Hazard. Mater. **424**, PD, 127670 (2022).
DOI: https://doi.org/10.1016/j.jhazmat.2021.127670

[6] A.N. Soon, B.H. Hameed, Heterogeneous catalytic treatment of synthetic dyes in aqueous media using Fenton and photo-assisted Fenton process. Desalination **269**, 1-3, 1-16 (2011).
DOI: https://doi.org/10.1016/j.desal.2010.11.002

[7] C. Lai et al., Enhancing iron redox cycling for promoting heterogeneous Fenton performance: A review. Sci. Total Environ.**775**, 145850 (2021).
DOI: https://doi.org/10.1016/j.scitotenv.2021.145850

[8] C. Wang, R. Jiang, J. Yang, P. Wang, Enhanced Heterogeneous Fenton Degradation of Organic Pollutants by CRC/Fe3O4 Catalyst at Neutral pH. Front. Chem. **10**, 1–8, (2022).
DOI: https://doi.org/10.3389/fchem.2022.892424

[9] F. Sun et al., A novel discovery of a heterogeneous Fenton-like system based on natural siderite: A wide range of pH values from 3 to 9. Sci. Total Environ. **698**, 34293 (2020).
DOI: https://doi.org/10.1016/j.scitotenv.2019.134293

[10] S. Eslaminejad, R. Rahimi, M. Fayazi, Sepiolite-metal organic framework-iron oxide catalyst for degradation of Rhodamine B using Fenton-like process. J. Taiwan Inst. Chem. Eng. **152**, 105181 (2023). DOI: https://doi.org/10.1016/j.jtice.2023.105181

[11] L. Duan, H. Jiang, W. Wu, D. Lin, K. Yang, Defective iron based metal-organic frameworks derived from zero-valent iron for highly efficient fenton-like catalysis. J. Hazard. Mater. **445**, 130426 (2023). DOI: https://doi.org/10.1016/j.jhazmat.2022.130426

[12] N.A. Zubir, C. Yacou, J. Motuzas, X. Zhang, J.C. Diniz Da Costa, Structural and functional investigation of graphene oxide-Fe 3 O 4 nanocomposites for the heterogeneous Fenton-like reaction. Sci. Rep. **4**, 1-8 (2014). DOI: https://doi.org/10.1038/srep04594

[13] N.A. Zubir, C. Yacou, J. Motuzas, X. Zhang, X.S. Zhao, J.C. Diniz Da Costa, The sacrificial role of graphene oxide in stabilising a Fenton-like catalyst GO-Fe3O4. Chem. Commun. **51**, 45, 9291-9293 (2015). DOI: https://doi.org/10.1039/c5cc02292d

[14] T. Wu, X. Li, C. Weng, F. Ding, F. Tan, R. Duan, Highly efficient LaMO3 (M=Co,Fe) perovskites catalyzed Fenton's reaction for degradation of direct blue 86. Environ. Res. **227**, 115756 (2023). DOI: https://doi.org/10.1016/j.envres.2023.115756

[15] R. Alrozi et al., Functional role of B-site substitution on the reactivity of CaMFeO3 (M = Cu, Mo, Co) perovskite catalysts in heterogeneous Fenton-like degradation of organic pollutant. J. Taiwan Inst. Chem. Eng. **143**, 104675 (2023).
DOI: https://doi.org/10.1016/j.jtice.2023.104675

[16] J. Li et al., Cobalt mediated perovskite as efficient Fenton-like catalysts for the tetracycline removal over a neutral condition: The importance of superoxide radical. Chemosphere **313**, November 2022, 137564 (2023).
DOI: https://doi.org/10.1016/j.chemosphere.2022.137564

[17] N.N.A. Abdul Rahman et al., B-site Substitution Effects on the Catalytic Activity of Perovskites Compounds towards Oxidative Degradation of Orange II Solutions. IOP Conf. Ser. Mater. Sci. Eng. **864**, 1 (2020).
DOI: https://doi.org/10.1088/1757-899X/864/1/012001

[18] Y. Rao et al., Enhanced peroxymonosulfate activation by Cu-doped LaFeO3 with rich oxygen vacancies: Compound-specific mechanisms. Chem. Eng. J. **435**, 134882 (2022).
DOI: https://doi.org/10.1016/j.cej.2022.134882

[19] L. Xie et al., Enhanced redox activity and oxygen vacancies of perovskite triggered by copper incorporation for the improvement of electro-Fenton activity. Chem. Eng. J. **428**, 131352 (2022).
DOI: https://doi.org/10.1016/j.cej.2021.131352

[20] P. Gao et al., Copper in LaMnO3 to promote peroxymonosulfate activation by regulating the reactive oxygen species in sulfamethoxazole degradation. J. Hazard. Mater. **411**, 125163 (2021).
DOI: https://doi.org/10.1016/j.jhazmat.2021.125163

[21] T. Chen et al., 3D hollow sphere-like Cu-incorporated LaAlO3 perovskites for peroxymonosulfate activation: Coaction of electron transfer and oxygen defect. Chem. Eng. J. **385**, 123935 (2020). DOI: https://doi.org/10.1016/j.cej.2019.123935

[22] K. Pan et al., Oxygen vacancy mediated surface charge redistribution of Cu-substituted LaFeO3 for degradation of bisphenol A by efficient decomposition of H2O2. J. Hazard. Mater. **389**, 122072 (2020). DOI: https://doi.org/10.1016/j.jhazmat.2020.122072

[23] X. Luo et al., Ordered Mesoporous Cobalt Containing Perovskite as a High-Performance Heterogeneous Catalyst in Activation of Peroxymonosulfate. ACS Appl. Mater. Interfaces **11**, 39, 35720-35728 (2019). DOI: https://doi.org/10.1021/acsami.9b11322

[24] C. Laurent et al., Beneficial effects of caffeine in a transgenic model of Alzheimer's Disease-like Tau pathology. Neurobiol. Aging **35**, 9, 2079-2090 (2014).
DOI: https://doi.org/10.1016/j.neurobiolaging.2014.03.027

[25] R.P. Barcelos, F.D. Lima, N.R. Carvalho, G. Bresciani, L.F. Royes, Caffeine effects on systemic metabolism, oxidative-inflammatory pathways, and exercise performance. Nutr. Res. **80**, 1-17 (2020). DOI: https://doi.org/10.1016/j.nutres.2020.05.005

[26] A. Pires et al., Long-term exposure of polychaetes to caffeine: Biochemical alterations induced in Diopatra neapolitana and Arenicola marina. Environ. Pollut. **214**, 456-463 (2016). DOI: https://doi.org/10.1016/j.envpol.2016.04.031

[27] M.A. Behnajady, N. Modirshahla, F. Ghanbary, A kinetic model for the decolorization of C.I. Acid Yellow 23 by Fenton process. J. Hazard. Mater. **148**, 1-2, 98-102 (2007). DOI: https://doi.org/10.1016/j.jhazmat.2007.02.003

[28] E. Bilgin Simsek, Ö. Tuna, Z. Balta, Construction of stable perovskite-type LaFeO3 particles on polymeric resin with boosted photocatalytic Fenton-like decaffeination under solar irradiation. Sep. Purif. Technol. **237**, 116384 (2020). DOI: https://doi.org/10.1016/j.seppur.2019.116384

[29] T. Hihara, Y. Okada, Z. Morita, Reactivity of phenylazonaphthol sulfonates, their estimation by semiempirical molecular orbital PM5 method, and the relation between their reactivity and azo-hydrazone tautomerism. Dye. Pigment. **59**, 3, 201-222 (2003). DOI: https://doi.org/10.1016/S0143-7208(03)00109-8

[30] J.A. Quintero-Jaramillo, J.I. Carrero-Mantilla, N.R. Sanabria-Gonzalez, A review of caffeine adsorption studies onto various types of adsorbents. Sci. World J. 2021, 1-18 (2021). DOI: https://doi.org/10.1155/2021/9998924

[31] J. Garcia-Ivars, M.I. Iborra-Clar, M. Massella, C. Carbonell-Alcaina, M.I. Alcaina-Miranda, Removal of pharmaceutically active compounds using low-pressure membrane processes. Desalin. Water Treat. **69**, 252-260 (2017). DOI: https://doi.org/10.5004/dwt.2017.0449

[32] L.Y. Liu, M. Pu, L. Yang, D.Q. Li, D.G. Evans, J. He, Experimental and theoretical study on the structure of acid orange 7-pillared layered double hydroxide. Mater. Chem. Phys. **106**, 422-427 (2007). DOI: https://doi.org/10.1016/j.matchemphys.2007.06.022

[33] J. Garcia-Ivars, L. Martella, M. Massella, C. Carbonell-Alcaina, M.I. Alcaina-Miranda, M.I. Iborra-Clar, Nanofiltration as tertiary treatment method for removing trace pharmaceutically active compounds in wastewater from wastewater treatment plants. Water Res. **125**, 360-373 (2017). DOI: https://doi.org/10.1016/j.watres.2017.08.070

[34] K.K. Beltrame, A.L. Cazetta, P.S.C. de Souza, L. Spessato, T.L. Silva, V.C. Almeida, Adsorption of caffeine on mesoporous activated carbon fibers prepared from pineapple plant leaves. Ecotoxicol. Environ. Saf. **147**, 64-71 (2018). DOI: https://doi.org/10.1016/j.ecoenv.2017.08.034

[35] C.V.T. Rigueto, M.T. Nazari, C.F. De Souza, J.S. Cadore, V.B. Brião, J.S. Piccin, Alternative techniques for caffeine removal from wastewater: An overview of opportunities and challenges. J. Water Process Eng. **35**, 101231 (2020). DOI: https://doi.org/10.1016/j.jwpe.2020.101231

[36] C.S. Santana, M.D. Nicodemos Ramos, C.C. Vieira Velloso, A. Aguiar, Kinetic Evaluation of Dye Decolorization by Fenton Processes in the Presence of 3-Hydroxyanthranilic Acid. Int. J. Environ. Res. Public Health **16**, 1602 (2019). DOI: https://doi.org/10.3390/ijerph16091602

[37] S. Haji, M. Khalaf, M. Shukrallah, J. Abdullah, S. Ahmed, A kinetic comparative study of azo dye decolorization by catalytic wet peroxide oxidation using Fe–Y zeolite/H2O2 and photooxidation using UV/H2O2. React. Kinet. Mech. Catal. **114**, 2, 795-815 (2015). DOI: https://doi.org/10.1007/s11144-014-0810-3

[38] N. Ertugay, F.N. Acar, Removal of COD and color from Direct Blue 71 azo dye wastewater by Fenton's oxidation: Kinetic study. Arab. J. Chem. **10**, S1158-S1163 (2017). DOI: https://doi.org/10.1016/j.arabjc.2013.02.009

[39] R. Santana, G. Nascimento, M.M.M.B. Duarte, Kinetic and eco-toxicological evaluation of the direct orange 26 dye degradation by Fenton and solar photo-Fenton processes. REGET/UFSM **22**, 1-20 (2021). DOI: https://doi.org/10.5902/2236117032254

[40] C.S. Santana, A. Aguiar, Effect of biological mediator, 3-hydroxy-anthranilic acid, in dye decolorization by Fenton processes. Int. Biodeterior. Biodegradation **104**, 1-7 (2015). DOI: https://doi.org/10.1016/j.ibiod.2015.05.007

[41] W. Chu, C.Y. Kwan, K.H. Chan, C. Chong, An unconventional approach to studying the reaction kinetics of the Fenton's oxidation of 2,4-dichlorophenoxyacetic acid. Chemosphere **57**, 1165-1171 (2004). DOI: https://doi.org/10.1016/j.chemosphere.2004.07.047

[42] E. Gürtekİn, M. Çelİk, E. Aydin, A. Çelİk, Degradation and mineralization of tetracycline by Fenton process. Environ. Res. Technol. **5**, 181-187 (2022). DOI: https://doi.org/10.35208/ert.1088757